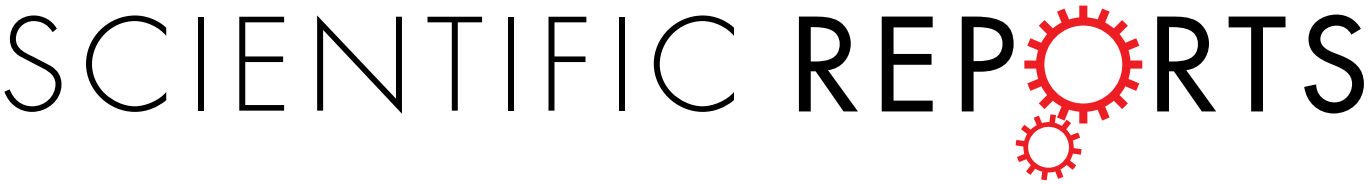

OPEN

The Effect of Excess Electron and hole on CO_2 Adsorption and Activation on Rutile (110) surface

Received: 13 January 2016
Accepted: 03 March 2016
Published: 17 March 2016

Wen-Jin Yin[1], Bo Wen[1], Sateesh Bandaru[1], Matthias Krack[2], MW Lau[1,3] & Li-Min Liu[1]

CO_2 capture and conversion into useful chemical fuel attracts great attention from many different fields. In the reduction process, excess electron is of key importance as it participates in the reaction, thus it is essential to know whether the excess electrons or holes affect the CO_2 conversion. Here, the first-principles calculations were carried out to explore the role of excess electron on adsorption and activation of CO_2 on rutile (110) surface. The calculated results demonstrate that CO_2 can be activated as CO_2 anions or CO_2 cation when the system contains excess electrons and holes. The electronic structure of the activated CO_2 is greatly changed, and the lowest unoccupied molecular orbital of CO_2 can be even lower than the conduction band minimum of TiO_2, which greatly facilities the CO_2 reduction. Meanwhile, the dissociation process of CO_2 undergoes an activated CO_2^- anion in bend configuration rather than the linear, while the long crossing distance of proton transfer greatly hinders the photocatalytic reduction of CO_2 on the rutile (110) surface. These results show the importance of the excess electrons on the CO_2 reduction process.

The increasing industrial growth has led to accelerated energy consumption especially the traditional fossil fuel, which inevitable releases amount of CO_2 that results in seriously global warming problem. It is of great urgency to reduce CO_2 emission, and this problem is gaining plenty of attentions from various fields[1–3]. In addition to the biological photosynthesis, different strategies such as physical and chemical approaches have been proposed to reduce and convert CO_2 to chemical fuels[4–6]. Photo-catalytic CO_2 conversion has been proved to be an efficient way to convert CO_2 by harnessing renewable solar energy, and it will generate synthetic fuels such as formaldehyde (HCHO), formic acid (HCOOH), methanol (CH_3OH), and methane (CH_4)[7–9].

Titanium dioxide (TiO_2) is considered as a model photocatalysis for CO_2 conversion as it is highly stable, non-toxic and cheap[10,11]. The early experiment proposed by Inoue *et al.*, reported that under UV light photo-catalytic reduction of CO_2 in the aqueous suspension of photosensitive semiconductor powders can form HCHO, HCOOH, CH_3OH, and CH_4 as main products[7]. Later, many efforts have been devoted to increase the efficiency and selectivity of the photo-catalytic CO_2 reduction[12–16]. The photo-catalytic CO_2 reduction results suggest that the catalytic activity can also be affected by TiO_2 phase, and they found that the brookite has a much higher activity than the anatase or rutile phase[17,18]. Further, the efficiency and selectivity of CO_2 reduction can be improved through doping noble metals, such as Pt, Pd, Cu, and Au atoms on TiO_2[19–22]. A previous report showed that the efficiency of CO_2 conversion into fuels can also be significantly affected by the hole-sacrifice, such as methanol[23]. Nonetheless, CO_2 can be successfully converted through photo-catalytic reduction, both the efficiency and selectivity of photo-catalytic system are still too low and poor for the realistic application. In order to design a more efficient and selective photo-catalyst, it is important to understand the detailed CO_2 reduction mechanism at the molecular level.

The photo-catalytic reduction of CO_2 into synthetic fuels is a multiple electron reaction process, which involves two-electron process to form CO and HCOOH, four-electron process to form HCHO, and eight-electron process to form CH_4[3,24–26]. For all these multiple electron reaction processes, the process starts initially from the adsorption and activation of CO_2 molecule, in which CO_2 involves configuration transformation, such as linear CO_2 to bent and proton transfer takes place. In real reaction process, the activation of CO_2 is a rate-limiting step[5]. CO_2 is a rather inert molecule with a positive electron affinity of 0.6 ± 0.2 eV[27]. Meanwhile, with respect to the normal hydrogen electrode (NHE), the reduction potential of CO_2/CO_2^- is about 1.9 eV, which is much higher

[1]Beijing Computational Science Research Center, Beijing 100084, China. [2]Paul Scherrer Institute, CH-5232 Villigen-PSI, Switzerland. [3]Chengdu Green Energy and Green Manufacturing Technology R&D Center, Chengdu, Sichuan, 610207, China. Correspondence and requests for materials should be addressed to L.-M.L. (email: limin.liu@csrc.ac.cn)

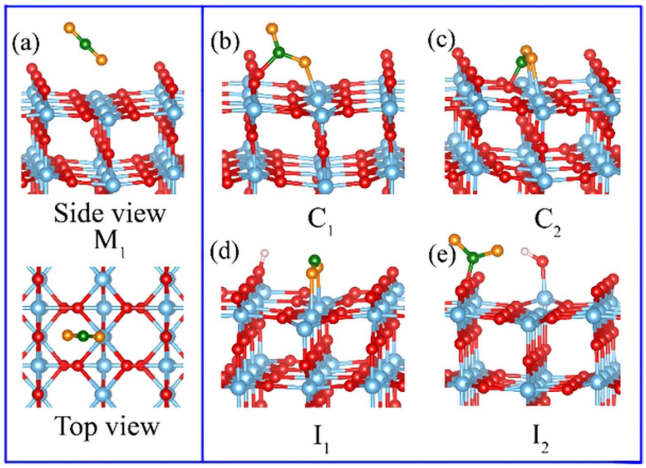

Figure 1. Different adsorption configurations of CO_2 adsorbed on excess electrons perfect rutile (110) surface. (**a**) M_1, molecular CO_2 adsorbs at five-fold Ti^{5f} in a tilted style. (**b**) C_1, one O atom of CO_2 bonds sits at the fivefold Ti^{5f}, and the C atom of CO_2 bonds with the bridge oxygen. (**c**) C_2, the two O atoms of CO_2 adsorb at two adjacent Ti^{5f} and the C atom bonding with the O^{3f} atom of TiO_2. (**d**) I_1, quite similar to C_2, while the C atoms does not interact with the surface oxygen atoms. (**e**) I_2, the C atom of CO_2 adsorbs on the top of the bridging oxygen in a tilted style. The O and Ti atoms in TiO_2 are represented in red and gray blue balls, while O and C atoms in CO_2 molecule are represented in orange and green balls.

than the TiO_2 conduction band minimum (CBM) about 0.4 eV above the Fermi level[28]. Thus, such relatively high potential prevents the efficient electron transfer process from TiO_2 to CO_2, which is a necessary for the photo-catalytic reduction reaction.

On the other side, several experiments have shown that the CO_2 can be triggered on the pure TiO_2[6,29]. The vibrational spectroscopic techniques have shown that CO_2^- anions is identified on pure TiO_2 surface, indicating electron can be transferred from TiO_2 to CO_2[23]. Additionally, Tan *et al.* found that CO_2 molecule can be activated by one electron and reduced to CO on the reduced rutile (110) surface based on scanning tunneling microscopy[30]. How to reconcile this paradox as most of the experimental results appear CO_2 can be converted, while lowest unoccupied molecular orbital (LUMO) value of CO_2 molecule is extremely high[28]. On the theoretical side, He *et al.* reported the CO_2^- anion is one of the important species on the charged anatase (101) surface, and the reduction of CO_2 into HCOOH or CO mainly it takes $2e^-$ reaction on anatase TiO_2(101)[31,32]. Thus, it is urgency to know how the excess electrons effect on the CO_2 adsorption and activation during the reduction process at the molecular level.

In this paper, we explore excess electrons effect on the structure and reactivity of CO_2 on the perfect and reduced rutile (110) by first-principles calculations. Spin moment and density calculations show that the CO_2 anion can exist in the TiO_2 (110) containing excess electrons, and a new configuration of CO_2 cation exists in the hole system. Furthermore, the electronic density of various CO_2 adsorptions show that the LUMO of CO_2 can be tuned by the excess electrons or hole. Especially, the LUMO of the activated CO_2 can even be lower than the TiO_2 CBM, which can effectively lower the reaction barrier. Our results show that the CO_2 activation and reduction processes on the rutile (110) surface are greatly affected by the excess electrons and holes.

Results

In the present study, we examine the effect of excess electrons on the CO_2 adsorption and activation on the perfect/reduced rutile (110) surfaces. We firstly focus on the role of excess electrons on the CO_2 adsorption configurations adsorbed on perfect rutile (110) surface. Later, intrinsic oxygen vacancy (O_v) defect is further explored. Further, we explore reaction pathway of CO_2 dissociation into CO on O_v rutile (110) surface and mechanism involves photo-catalytic reduction of CO_2 to form a HCOOH.

The excess electrons effect on CO_2 adsorption on the perfect rutile (110) surface. In this section, we initially focus on the possible CO_2 adsorption configurations in the case of excess electrons on the perfect rutile (110) surface. Before discussing the detailed CO_2 adsorption, it should be emphasized that the linear molecular CO_2 is firstly physically adsorbed on the rutile (110) surface. And according to the previous our results[33], the molecular CO_2 linearly adsorbed at five-fold Ti^{5f} in a tilted style is the most stable one. Based on this adsorption, the molecular CO_2 will undergo a translation into bend through activation or reduction. As a result, the molecular adsorbed CO_2 changes to the bend chemical adsorption. Five different binding configurations of CO_2 exist on rutile (110) surface. All possible adsorption configurations are examined, which are labeled as M_1, C_1, C_2, I_1 and I_2 (see Fig. 1). M_1 is a physical adsorption, where the CO_2 linearly adsorbs at five-fold Ti^{5f} in a tilted style. Except M_1, all other four C_1, C_2 and I_1, I_2 configurations are chemical adsorptions: In C_1 configuration, one O atom of CO_2 bonds to the fivefold Ti^{5f}, and the C atom of CO_2 interacts with the bridge oxygen, forming a bent CO_2 configuration; As for C_2, the two O atoms of CO_2 adsorbs at two adjacent Ti^{5f} sites, and the C atom directly bonds with the

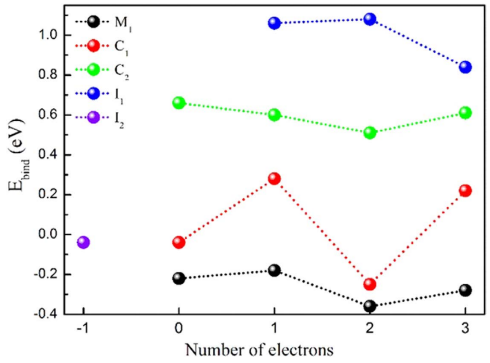

Figure 2. The binding energy of the CO_2 adsorptions vs the different number of excess electrons in prefect rutile (110) surface. The positive digit denotes the number of excess electrons, and the negative digit means the number of hole in the transverse axis. Here the negative value indicates relatively large adsorption energy.

Parameter	M_1	C_1	C_2	I_1	I_2
Ti-O (Å)	2.60	1.94	2.16	2.13	
C-O (Å)	1.16	1.32	1.26	1.25	1.26
O-C-O (θ)	177.6	127.2	132.5	135.0	120.2
Net Charge (e)	0.05	−0.29	−0.29	−0.29	−0.05
Spin (μ_B)	0	0	0	0.74	0.90
Parameter	**CO_2**	**Ov-1**	**Ov-2**	**Ov-3**	**Ov-4**
Ti-O (Å)		2.67	2.23	2.15	2.70
C-O (Å)	1.18	1.19	1.28	1.29	1.34
O-C-O (θ)	180.0	179.8	132.9	129.3	129.3
Net Charge (e)	0	0.06	−0.41	−0.43	−0.35
Spin (μ_B)	0	0	0.82	0	0
E_{bind} (eV)		−1.08	−0.16	−0.83	−1.11

Table 1. Representative geometrical parameters, net charge, spin polarized moment for the CO_2 adsorbed on excess electron perfect (M_1, C_1, C_2, I_1, and I_2) and reduce rutile (110) ($O_{v\text{-}1}$, $O_{v\text{-}2}$, $O_{v\text{-}3}$, and $O_{v\text{-}4}$) surface. The binding energy for CO_2 on reduced TiO_2 is also included.

O^{3f} atom of TiO_2; Quite similar to C_2, the C atom of I_1 does not interact with surface oxygen atom; As for I_2, the CO_2 adsorbs on the top of the bridging oxygen, forming a new C-O^{2f} bond.

In Fig. 2, the positive digit in the transverse axis represents the number of excess electron, while the negative digit denotes the number of hole. When the system does not contain any excess electron or hole, three different binding configurations of CO_2 on the perfect TiO_2 were identified after the geometry relaxation, namely M_1, C_1 and C_2. The others, I_1 and I_2, are unstable. The corresponding binding energy shows that M_1 has the largest binding energy of −0.23 eV as the system does not contain excess electron, which is a little smaller than the earlier reported pure PBE value of −0.35 eV[33,34]. This is because PBE+U functional treats the d-orbital of Ti in a more localization.

As an electron is introduced to TiO_2, I_1 can exist with a binding energy of 1.02 eV. Therefore, the CO_2 adsorption in I_1 is meta-stable. It should be noted that the same kind configuration is also reported on the anatase (101) surface, and the corresponding adsorption energy of CO_2 is 0.78 eV[31], which is quite close the current one. When more electrons are included in TiO_2, no new configuration appears, and the corresponding binding energy are also not sensitive to the number of excess electrons. When the TiO_2 surface is charged with holes, the configuration of I_2 can exist with a binding energy of −0.05 eV.

The detailed geometrical parameters, net charge, and spin polarized moment of the CO_2 adsorption configurations are also calculated as shown in Table 1. Among these five states, the configurations of M_1, C_1 and C_2 adsorbed on the perfect without excess electron or hole are chosen as they are not sensitive to the excess electrons. While the configurations of I_1 and I_2 are shown for the system containing one electron or hole. Compared with the single CO_2 molecule, the C-O bond length of CO_2 in M_1 is almost similar, and the ∠O-C-O angle slightly decreases by 2.38°. The net charge and spin polarized moment of adsorbed CO_2 are the same to that of single CO_2 molecule. A keen look into the structures of the C_1/C_2, the C-O bond length in C_1/C_2 increases by 0.08/0.14 Å, while the ∠O-C-O bond angle decreases by 53.76/47.45°. In case of C_1 and C_2, owing to the strong interaction between the CO_2 and rutile (110) surface, charge transfer occurs from TiO_2 to CO_2 by about 0.29e^-. The spin polarized moment of these two adsorbed CO_2 states is zero, demonstrating that there is no unpaired electron existing in both C_1 and C_2.

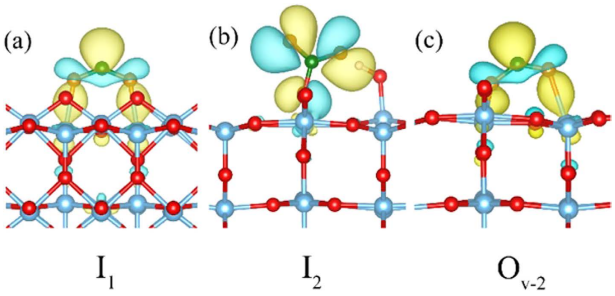

Figure 3. Spin densities of different binding configurations of CO_2 on excess electrons perfect and O_v rutile (110) surface. Spin density of (**a**) I_1 with an excess electron and (**b**) I_2 with an hole on the perfect rutile (110) surface. (**c**) spin density of O_{v-2} on the reduced rutile (110) surface.

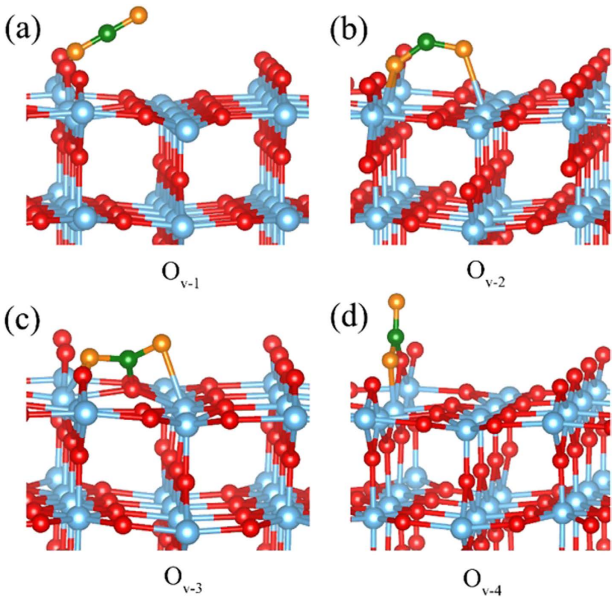

Figure 4. Different adsorption configurations of CO_2 on O_v rutile (110) surface. (**a**) O_{v-1}, CO_2 molecule adsorbed at O_v site in a titled style. (**b**) O_{v-2}, one O of CO_2 adsorbed at O_v site and the other O adsorbed at Ti^{5f} in the plane. (**c**) O_{v-3}, quite similar to O_{v-2} except for the C atom linked to O^{3f} in the plane. (**d**) O_{v-4}, one O atom of CO_2 adsorbed at O_v site and the C atom adsorbed with the O^{2f} near the O_v site.

As we mentioned above, when the system contains the excess electron, the I_1 becomes metastable. As for the I_1, the relaxed geometric parameters (Ti-O, C-O and ∠O-C-O) of I_1 and net charges are quite close to C_2, but the spin polarized moment is 0.74 μ_B, indicating an unpaired electron is located on the CO_2 forming a activated state of I_1. The corresponding spin densities as shown in Fig. 3. The excess electron is mainly localized on the C atom of the CO_2, suggesting that an excess electron is transferred from TiO_2 to CO_2 and to form a CO_2^- anion[31]. It should be mentioned that although this configuration is rather unfavorable, the extra electron is shown to be critical to stabilize this binding configuration. When it comes to I_2, the C-O bond length is little elongated to 1.27 Å, and the ∠O-C-O angle enormously decreases to 120.27°. The spin polarized moment is about 0.90 μ_B, indicating an unpaired electron is located on CO_2. Further spin density calculation demonstrates that the electron in I_2 is localized at the two O atoms instead of C atom in the CO_2 forming a activated CO_2^+ cation as shown in Fig. 3, which is different from the previous reported result only forming CO_2^- state[31]. From the above results, we clearly observe that various CO_2 adsorptions appear on the perfect rutile (110) surface in the case of excess electrons or holes.

CO_2 adsorption on O_v rutile (110) surface. Apart from excess electron on the perfect TiO_2 case, the intrinsic oxygen vacancy (O_v) defect can also provide two excess electrons to the rutile TiO_2(110)[35]. Here, we consider one O_v defect in rutile (110) surface to simulate the effect of excess electrons on the CO_2 adsorption. Relative to the above perfect TiO_2, O_v defect not only provides the excess electrons but also the adsorption sites.

Here, four different configurations are examined, labeled as $O_{v-1} \sim O_{v-4}$ as shown in Fig. 4. O_{v-1} linearly adsorbs in the middle of O_v in a tilted configuration. In case of O_{v-2}, one of the O atom of CO_2 binds to two 5-fold Ti atoms (Ti^{5f}) in the O_v site through bi-dentate fashion, while the other "O" atom interacts with the 5-fold Ti atom (Ti^{5f}) in the plane. The configuration of O_{v-3} is quite close to O_{v-2} except for the C atom linked to the 3-fold "O" atom (O^{3f})

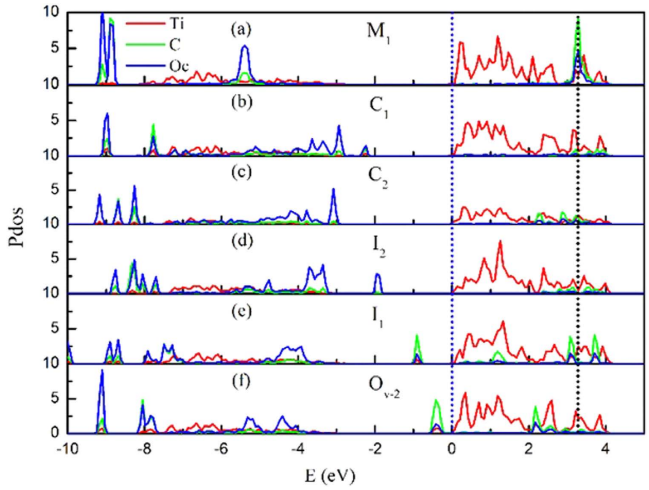

Figure 5. The partial density of states (PDOS) of the different CO_2 adsorption configurations on the excess electrons rutile (110) surface. (**a**) PDOS for the molecular CO_2 adsorption state M_1, and (**b**)/(**c**) corresponds to bending adsorption state C_1/C_2. (**d**,**e**) PDOS for I_2 with an hole and I_1 with an excess electron, respectively. (**f**) PDOS for $O_{v\text{-}2}$ adsorbed on reduced rutile (110). The plots in red is the PDOS of the single Ti atom adsorbed by the CO_2. The plots in green and blue are the C atom and O atom of the adsorbed CO_2, respectively.

in the plane; the CO_2 in $O_{v\text{-}4}$ adsorbs in the bridging oxygen row with the O mono-dentate adsorbed to Ti^{5f} in O_v site and C atom bonds to bridging oxygen O^{2f}.

The corresponding binding energies, geometrical parameters, net charge, and spin polarized moment of the CO_2 adsorption on reduced TiO_2 are also summarized in Table 1. Previous theoretical result shows that the CO_2 interacting with $O_{v\text{-}4}$ configuration on the anatase (101) cluster is the most stable adsorption with the binding energy of −1.09 eV[31]. Similarly, the calculated binding energy of CO_2 in $O_{v\text{-}4}$ has the highest binding energy of −1.11 eV in our present study, indicates that $O_{v\text{-}4}$ is indeed more favorable adsorption. The binding energy of $O_{v\text{-}1}$ is about −1.08 eV, which is quite close to $O_{v\text{-}4}$, suggesting that $O_{v\text{-}1}$ is also relatively stable configuration. The other two configurations $O_{v\text{-}2}$ and $O_{v\text{-}3}$ have relatively lower binding energies than $O_{v\text{-}1}$ and $O_{v\text{-}4}$, indicating that they are meta-stable.

A keen look into the geometrical parameters of $O_{v\text{-}1}$~$O_{v\text{-}4}$, the CO_2 in $O_{v\text{-}1}$ configuration both bond lengths and angles are very close to the isolated CO_2 molecule (Table 1). Unlike the $O_{v\text{-}1}$, the bond length of C-O in $O_{v\text{-}2}$~$O_{v\text{-}4}$ is elongated by 0.1–0.16 Å, and the angle ∠O-C-O significantly decreases by ∠47.05–50.68° compared with an isolated CO_2 molecule. Similar to C_1 and C_2 on perfect TiO_2 (110), net charge of $O_{v\text{-}2}$~$O_{v\text{-}4}$ is about $-0.41e^-$, suggesting that charge redistribution between CO_2 and TiO_2. Most strikingly, spin polarized moment studies shows that the $O_{v\text{-}1}$, $O_{v\text{-}3}$, and $O_{v\text{-}4}$ the calculated spin moments are equal to zero, whereas $O_{v\text{-}2}$ has a spin moment of 0.82 μ_B, indicating an electron is located in the CO_2. Further spin density calculation reveals that the electron is localized on the C atom of the CO_2 as shown in Fig. 3. Thus, the CO_2 in $O_{v\text{-}2}$ indeed converts into an activated CO_2^- anion. Although $O_{v\text{-}2}$ has a relatively lower binding energy than other configurations, the extra electron at "C" atom is crucial to stabilize the binding configuration.

It is well known that the LUMO value of an isolated CO_2 molecule is very high, and the electron is very difficult to transfer to the CO_2 molecule from the TiO_2 conduction band[3]. In order to know whether the above CO_2 adsorptions can affect the LUMO of CO_2 in the presence of excess electron or hole, the partial density of states (PDOS) of the adsorbed CO_2 is calculated. The results are shown in Fig. 5. As for M_1, the LUMO value is located above the TiO_2 CBM onset by 3.4 eV. This value is in consistent with the estimated value of 3.5 eV by Indrakanti *et al.*, and a little larger than the value of 2.3 eV by Tan *et al.*[3,30] .Thus, the electron in the TiO_2 CBM is rather difficult to be transferred to the CO_2 in molecular state. When the CO_2 is changed to bending adsorption configurations (C_1 and C_2), the localized LUMO of CO_2 molecule becomes delocalized state, and the LUMO onset shifts down to 2.3 eV. Therefore, the energy level can be modified by CO_2 adsorption mode. Whereas this value is still too large for the electron transfer from the TiO_2 conduction band to the CO_2 molecule. When the CO_2 adsorptions with the configurations of I_1, I_2, and $O_{v\text{-}2}$ on TiO_2 (110) containing excess electron or hole, the PDOS shows the LUMO of CO_2 shifts further downward, which can even be lower than the TiO_2 CBM. Hence, the electron or hole can easily transfer from TiO_2 CBM to the CO_2 with I_1, I_2, and $O_{v\text{-}2}$.

Dissociation of CO_2 into CO on O_v rutile (110) surface. As discussed above, the CO_2 adsorption on the O_v rutile (110) surface can be activated, and the corresponding LUMO is even lower than TiO_2 CBM. Thus it is interesting to know how the CO_2 adsorption on O_v rutile (110) can be further converted into the other species. The activation process can be expressed as:

$$CO_2 + e^- \rightarrow CO_2^- \quad (1)$$

From the equation (2), we can clearly observe that the activation of CO_2 process needs an excess electron in the system. Scanning tunneling microscopy experiment suggested that the conversion of CO_2 to CO is relative to

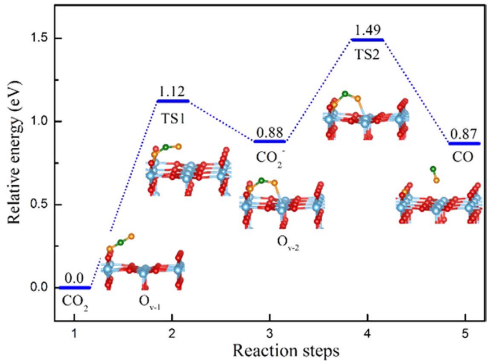

Figure 6. Illustration of reaction pathway via O_{v-2} configuration to form CO. The sum energy of the CO_2 and O_v rutile TiO_2 is the zero reference for energy.

electron attachment state of linear CO_2 molecule on the O_v rutile (110) surface[30]. However, the detailed dissociation of CO_2 mechanism at molecular level is still unknown. Here, we start the study from configuration O_{v-1} with intrinsic excess electrons in reduced TiO_2, and the dissociation of CO_2 into CO are explored. The detailed reaction pathway and calculated energy barriers are shown in Fig. 6.

As shown in Fig. 6, the CO_2 molecule firstly adsorbs at the oxygen vacancy, forming the linear adsorption as O_{v-1}. In this step, there is no electron transfer from reduced TiO_2 to linear CO_2, which is a different from the previous result where the linear CO_2 can form an electron attachment state[36]. Then, the linear adsorbed CO_2 molecule initiates to bent, which undergoes a transition state transition state 1 (TS1) with an energy barrier 1.12 eV to form O_{v-2} structure. Subsequently, the excess electron in the TiO_2 transfers to the CO_2, forming CO_2^- anion (see Fig. 3). On the basis of CO_2^- anion, the C-O bond breaks to form CO, leaving an O atom at the oxygen vacancy site. The energy barrier of this process is about 0.61 eV. From the whole process, the CO formation undergoes an activation state of O_{v-2} rather than a direct C-O bond breaking of linear CO_2.

Photo-catalytic reduction of CO_2 to form HCOOH. Apart from the CO formation in the reduced TiO_2, photo-catalytic reduction of CO_2 can also form synthetic fuels such as formaldehyde (HCHO), formic acid (HCOOH), methanol (CH_3OH), and methane (CH_4) on the TiO_2 based materials. However, the formation of these useful fuels through activated CO_2 is still rare, and most of the theoretical researches mainly focus on the anatase phase[32]. Here, on the basis of configuration I_1, the reduction of CO_2 to form HCOOH is investigated, which can be expressed as:

$$CO_2 + e^- \rightarrow CO_2^- \quad (2)$$

$$CO_2^- + H^+ + e^- \rightarrow HCO_2^- \quad (3)$$

$$HCO_2^- + H^+ \rightarrow HCOOH \quad (4)$$

From equations (3) to (5), we can clearly understand that the reaction involves two electrons and two protons in the system. The complete reduction process can be divided into five steps as follows: The molecular CO_2 firstly adsorbs on the rutile (110) surface as C_1; Following this, excess electron injects into CO_2, and the corresponding CO_2 becomes CO_2^- anion as I_1; Then, one proton and electron transfer to the CO_2^- anion, forming HCO_2^-; Finally, the other proton transfers to HCO_2^-, forming HCOOH.

According to the above reaction processes, the transition states and corresponding energy barriers of CO_2 reduction to HCOOH are summarized in Fig. 7. On the basis of configuration C_1, the two O atoms of CO_2 begin to bend towards the adjacent fivefold Ti^{5f} in plane through TS1, the two O atoms of CO_2 is adsorbed by Ti^{5f} in nature as shown step-3 in Fig. 7. Consecutively, the electron spontaneously transfers to the CO_2 forming the CO_2^- anion. This process needs to overcome an energy barrier of 1.28 eV, which is much higher than the case in anatase (101) of 0.87 eV[32]. Consecutive proton and electron move to the "C" atom of CO_2^- anion to form HCO_2^-. These findings are very different from the case in anatase (101). In anatase case, proton transfer occurs with no energy barrier, but the proton transfer on rutile needs to overcome an energy barrier of 0.93 eV. The calculated energy barrier is relatively higher, because the proton should move about 3.10 Å between the adsorbed proton and the CO_2^- anion, which is larger than the one in anatase (about 2.60 Å). Further, the other proton moves to the "O" atom of HCO_2^-, resulting in HCOOH. This process needs a moderate energy barrier of 0.75 eV. From the complete reduction process, the formation of CO_2^- anion is the rate limiting step, and also the proton transfer step is much difficult than the earlier reported anatase (101) surface[32].

Activation of CO_2 by a hole. On the basis of configuration I_2, the activation of CO_2 by the hole is also investigated, which can be expressed as:

$$CO_2 + h^+ \rightarrow CO_2^+ \quad (5)$$

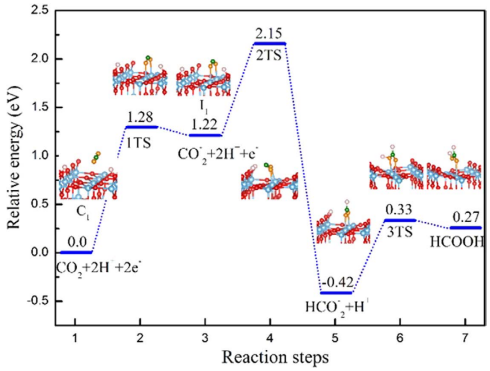

Figure 7. Illustration of reaction pathway via I_1 configuration to form HCOOH. The sum of energies of the CO_2 and 2H is the zero reference for energy. The sign of " + " indicates non-interacting species (e.g. $CO_2 + OH$), and the transition state denotes by TS.

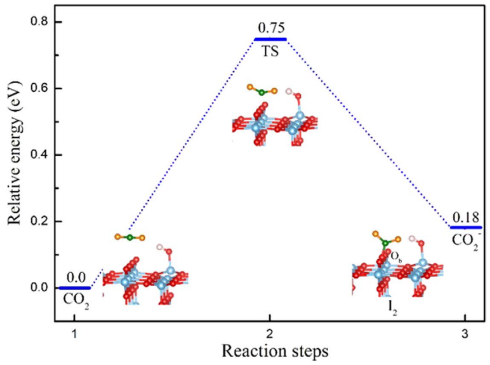

Figure 8. Illustration of reaction pathway to form CO_2^+ cation. The sum energy of CO_2 and TiO_2 is set to zero as the reference energy.

In the CO_2 activation process (Eq. 6), a hole is transferred to the O atom of CO_2 in configuration I_2. The detailed reaction process and activation barrier of hole to CO_2 with I_2 are calculated (Fig. 8). The molecular CO_2 adsorbs on the top of bridge oxygen on TiO_2 with a C-O_b distance of 2.71 Å. Then the C atom of the CO_2 moves towards the bridge-site oxygen. In the transition state geometry, the C-O_b distance decreases from 2.71 Å to 1.74 Å. Finally, the "C" atom of CO_2 adsorbed with the bridge oxygen forming a bent like CO_2, and the C-O_b distance decreases to 1.34 Å. Simultaneously, the hole is transferred to the two "O" atoms of CO_2 forming a CO_2^+ as shown in Fig. 3. Formation of cation need to overcome a relatively lower energy barrier (about 0.75 eV) than that of anions.

Discussions

In summary, by the first-principles calculations, structural and reactivity behavior of CO_2 on rutile TiO_2 are greatly affected by excess electrons. The computed results show that various CO_2 adsorption configurations appear in the case of excess electrons, and activated CO_2 adsorption configurations can be exist in the not only excess electron system as I_1 and $O_{v\text{-}2}$, but also in the hole system as I_2. Further electronic density calculation shows that the LUMO of CO_2 can be modified by varying the CO_2 adsorption states, and it can even be lowered and below the TiO_2 conduction band. The detailed CO_2 activation and reduction processes are also explored. The mechanism of CO_2 reduction to CO on oxygen vacancy rutile (110) surface is revised, the reduction process involves the formation of CO_2 anion in bend type structure with an energy barrier of 1.12 eV. The results also suggest that, the energy barrier of rate limitation step to form HCOOH is about 1.28 eV. In addition, the process for the formation of CO_2^+ cation in the hole system is also investigated, and it needs a much lower energy barrier of 0.75 eV.

Method

The calculations are performed based on the spin-polarized density functional theory (DFT) in periodic boundary conditions, as implemented in the CP2K/Quickstep package[37]. This simulation code employs hybrid Gaussian and plane wave (GPW) basis sets and norm conserving Goedecker-Teter-Hutter (GTH) pseudo-potentials to represent the ion-electron interactions[38,39]. The Gaussian functions consisting of a double-ζ plus polarization (DZVP) basis set was employed to optimize the structures[40]. The energy cutoff for the real space grid was 500 Ry, which yields total energies converged to at least 0.001 eV per atom. For the exchange-correlation functional, we have used the Perdew-Burke-Ernzerhof (PBE) functional of generalized gradient approximation (GGA)[41]. The

vdW correction is considered with the Grimme approach (DFT-D3)[42]. Since the standard GGA functional has the limitation to calculate the d-band electrons of transition metal, GGA+U functional is used to treat Ti 3d electron with U = 4.2 eV[43]. In order to avoid the interaction between the adjacent images, a vacuum spacing of 15 Å is employed for all the systems. Transition states along the reaction pathways are searched by the Climbing Image Nudged Elastic Band (CI-NEB) approach[44].

The interaction between the adsorbed molecule and the substrate, which can be characterized by the binding energy, which is defined as,

$$E_b = E_{ab/sub} - E_{ad} - E_{sub} \quad (6)$$

where $E_{ad/sub}$ is the total energy of the molecule adsorbed on the substrate, E_{ad} is the energy of the isolated molecule in the same box, and the E_{sub} is the energy of the substrate. In the present study, a (4×2) supercell is used to represent rutile TiO_2 (110) substrate containing four tri-layers. In the rutile TiO_2(110) features three types of under coordinated atoms: five-fold Ti ionic (Ti^{5f}), bridge oxygen atom in two-fold (O^{2f}), and planar three-fold oxygen atom (O^{3f}). The excess electrons in the system are simulated by adding hydrogen atoms or hydroxyls, and one hydrogen/hydroxyl corresponds to one electron/hole[45]. All the CO_2 adsorption configurations studied in the text, only one CO_2 molecule is considered to adsorb on the (4×2) supercell, corresponding to 1/8 ML coverage.

References

1. Tu, W., Zhou, Y. & Zou, Z. Photocatalytic Conversion of CO_2 into Renewable Hydrocarbon Fuels: State-of-the-Art Accomplishment, Challenges, and Prospects. *Adv Mater* **26,** 4607–4626, doi: 10.1002/adma.201400087 (2014).
2. Dhakshinamoorthy, A., Navalon, S., Corma, A. & Garcia, H. Photocatalytic CO_2 reduction by TiO_2 and related titanium containing solids. *Energ Environ Sci* **5,** 9217–9233, doi: 10.1039/c2ee21948d (2012).
3. Indrakanti, V. P., Kubicki, J. D. & Schobert, H. H. Photoinduced activation of CO_2 on Ti-based heterogeneous catalysts: Current state, chemical physics-based insights and outlook. *Energ Environ Sci* **2,** 745–758, doi: 10.1039/b822176f (2009).
4. Liu, L. J. & Li, Y. Understanding the Reaction Mechanism of Photocatalytic Reduction of CO_2 with H_2O on TiO_2-Based Photocatalysts: A Review. *Aerosol Air Qual Res* **14,** 453–469, doi: 10.4209/aaqr.2013.06.0186 (2014).
5. Burghaus, U. Surface chemistry of CO_2 – Adsorption of carbon dioxide on clean surfaces at ultrahigh vacuum. *Prog. Surf. Sci.* **89,** 161–217, doi: 10.1016/j.progsurf.2014.03.002 (2014).
6. Krischok, S., Hofft, O. & Kempter, V. The chemisorption of H_2O and CO_2 on TiO_2 surfaces: studies with MIES and UPS (HeI/II). *Surf. Sci.* **507,** 69–73, doi: 10.1016/S0039-6028(02)01177-9 (2002).
7. Inoue, T., Fujishima, A., Konishi, S. & Honda, K. Photoelectrocatalytic reduction of carbon dioxide in aqueous suspensions of semiconductor powders. *Nature* **277,** 637–638, doi: 10.1038/277637a0 (1977).
8. Dimitrijevic, N. M. *et al.* Role of water and carbonates in photocatalytic transformation of CO_2 to CH_4 on titania. *J. Am. Chem. Soc.* **133,** 3964–3971, doi: 10.1021/ja108791u (2011).
9. Yu, J., Low, J., Xiao, W., Zhou, P. & Jaroniec, M. Enhanced Photocatalytic CO_2-Reduction Activity of Anatase TiO_2 by Coexposed {001} and {101} Facets. *J. Am. Chem. Soc.* **136,** 8839–8842, doi: 10.1021/ja5044787 (2014).
10. Schneider, J. *et al.* Understanding TiO_2 photocatalysis: mechanisms and materials. *Chem. Rev.* **114,** 9919–9986, doi: 10.1021/cr5001892 (2014).
11. Ma, Y., Wang, X., Chen, X., Han, H. & Li, C. Titanium Dioxide-Based Nanomaterials for Photocatalytic Fuel Generations. *Chem. Rev.* **114,** 9987–10043, doi: 10.1021/cr500008u (2014).
12. Henderson, M. A. Evidence for bicarbonate formation on vacuum annealed TiO_2(110) resulting from a precursor-mediated interaction between CO_2 and H_2O. *Surf. Sci.* **400,** 203–219, doi: 10.1016/S0039-6028(97)00863-7 (1997).
13. Lo, C. C., Hung, C. H., Yuan, C. S. & Wu, J. F. Photoreduction of carbon dioxide with H_2 and H_2O over TiO_2 and ZrO_2 in a circulated photocatalytic reactor. *Sol Energ Mat Sol C* **91,** 1765–1774, doi: 10.1016/j.solmat.2007.06.003 (2007).
14. Varghese, O. K., Paulose, M., LaTempa, T. J. & Grimes, C. A. High-Rate Solar Photocatalytic Conversion of CO_2 and Water apor to Hydrocarbon Fuels. *Nano letters* **9,** 731–737, doi: 10.1021/nl803258p (2008).
15. Indrakanti, V. P., Kubicki, J. D. & Schobert, H. H. Quantum Chemical Modeling of Ground States of CO_2 Chemisorbed on Anatase (001), (101), and (010) TiO_2 Surfaces. *Energ Fuel* **22,** 2611–2618, doi: 10.1021/ef700725u (2008).
16. Roy, S. C., Varghese, O. K., Paulose, M. & Grimes, C. A. Toward Solar Fuels: Photocatalytic Conversion of Carbon Dioxide to Hydrocarbons. *Acs Nano* **4,** 1259–1278, doi: 10.1021/nn9015423 (2010).
17. Liu, L., Zhao, H., Andino, J. M. & Li, Y. Photocatalytic CO_2 Reduction with H_2O on TiO_2 Nanocrystals: comparison of Anatase, Rutile, and Brookite Polymorphs and Exploration of Surface Chemistry. *ACS Catal.* **2,** 1817–1828, doi: 10.1021/cs300273q (2012).
18. Rodriguez, M. M., Peng, X., Liu, L., Li, Y. & Andino, J. M. A Density Functional Theory and Experimental Study of CO_2 Interaction with Brookite TiO_2. *J. Phys. Chem. C* **116,** 19755–19764, doi: 10.1021/jp302342t (2012).
19. Yui, T. *et al.* Photochemical reduction of CO_2 using TiO_2: effects of organic adsorbates on TiO_2 and deposition of Pd onto TiO_2. *ACS Appl. Mater. Interfaces* **3,** 2594–2600, doi: 10.1021/am200425y (2011).
20. Yamashita, H., Nishiguchi, H., Kamada, N. & Anpo, M. Photocatalytic Reduction Of Co_2 With H_2o On Tio_2 And Cu/Tio_2 Catalysts. *Res. Chem. Intermed* **20,** 815–823, doi: 10.1163/156856794X00568 (1994).
21. Sen, S., Liu, D. & Palmore, G. T. R. Electrochemical Reduction of CO_2 at Copper Nanofoams. *ACS Catal.* **4,** 3091–3095, doi: 10.1021/cs500522g (2014).
22. Xie, S., Wang, Y., Zhang, Q., Fan, W. & Deng, W. Photocatalytic reduction of CO_2 with H_2O: significant enhancement of the activity of Pt-TiO_2 in CH_4 formation by addition of MgO. *Chem. Commun.* **49,** 2451–2453, doi: 10.1039/c3cc00107e (2013).
23. Ulagappan, N. & Frei, H. Mechanistic Study of CO_2 Photoreduction in Ti Silicalite Molecular Sieve by FT-IR Spectroscopy. *J. Phys. Chem. A* **104,** 7834–7839, doi: 10.1021/jp001470i (2000).
24. Mori, K., Yamashita, H. & Anpo, M. Photocatalytic reduction of CO_2 with H_2O on various titanium oxide photocatalysts. *RSC Adv.* **2,** 3165, doi: 10.1039/c2ra01332k (2012).
25. Lee, J., Sorescu, D. C. & Deng, X. Electron-induced dissociation of CO_2 on TiO_2(110). *J. Am. Chem. Soc.* **133,** 10066–10069, doi: 10.1021/ja204077e (2011).
26. Pipornpong, W., Wanbayor, R. & Ruangpornvisuti, V. Adsorption CO_2 on the perfect and oxygen vacancy defect surfaces of anatase TiO_2 and its photocatalytic mechanism of conversion to CO. *Appl. Surf. Sci.* **257,** 10322–10328, doi: 10.1016/j.apsusc.2011.06.013 (2011).
27. Sommerfeld, T., Meyer, H. D. & Cederbaum, L. S. Potential energy surface of the CO_2^- anion. *Phys. Chem. Chem. Phys.* **6,** 42–45, doi: 10.1039/b312005h (2004).
28. Indrakanti, V. P., Schobert, H. H. & Kubicki, J. D. Quantum Mechanical Modeling of CO_2 Interactions with Irradiated Stoichiometric and Oxygen-Deficient Anatase TiO_2 Surfaces: Implications for the Photocatalytic Reduction of CO_2. *Energ Fuel* **23,** 5247–5256, doi: 10.1021/ef9003957 (2009).

29. Acharya, D. P., Camillone, N. & Sutter, P. CO_2 Adsorption, Diffusion, and Electron-Induced Chemistry on Rutile TiO_2(110): A Low-Temperature Scanning Tunneling Microscopy Study. *J. Phys. Chem. C* **115,** 12095–12105, doi: 10.1021/jp202476v (2011).
30. Tan, S. *et al.* CO_2 dissociation activated through electron attachment on the reduced rutile TiO_2(110)-1 × 1 surface. *Phys. Rev. B* **84,** 155418(1)-155418(5), doi: 10.1103/PhysRevB.84.155418 (2011).
31. He, H. Y., Zapol, P. & Curtiss, L. A. A Theoretical Study of CO_2 Anions on Anatase (101) Surface. *J. Phys. Chem. C* **114,** 21474–21481, doi: 10.1021/jp106579b (2010).
32. He, H., Zapol, P. & Curtissa, L. A. Computational screening of dopants for photocatalytic two-electron reduction of CO_2 on anatase (101) surfaces. *Energ Environ Sci* **5,** 6196–6205, doi: 10.1039/c2ee02665a/ (2012).
33. Yin, W. J., Krack, M., Wen, B., Ma, S. & Liu, L. CO_2 Capture and Conversion on Rutile TiO_2(110) in the Water Environment: Insight by First-Principles Calculations. *J. Phys. Chem. Lett*, 2538–2545, doi: 10.1021/acs.jpclett.5b00798 (2015).
34. Sorescu, D. C., Lee, J., Al-Saidi, W. A. & Jordan, K. D. Coadsorption properties of CO_2 and H_2O on TiO_2 rutile (110): a dispersion-corrected DFT study. *J. Chem. Phys.* **137,** 074704(1)-074704(16), doi: 10.1063/1.4739088 (2012).
35. Sun, C., Liu, L. M., Selloni, A., Lu, G. & Smith, S. C. Titania-water interactions: a review of theoretical studies. *J. Mater. Chem.* **20,** 10319, doi: 10.1039/c0jm01491e (2010).
36. Tan, S. *et al.* CO_2 dissociation activated through electron attachment on the reduced rutile TiO2(110)-1 × 1 surface. *Phys. Rev. B* **84,** 155418(1)-155418(5), doi: 10.1103/PhysRevB.84.155418 (2011).
37. Vondele, V. *et al.* Quickstep: Fast and accurate density functional calculations using a mixed Gaussian and plane waves approach. *Comput. Phys. Commun.* **167,** 103–128, http://dx.doi.org/10.1016/j.cpc.2004.12.014 (2005).
38. Goedecker, S., Teter, M. & Hutter, J. Separable dual-space Gaussian pseudopotentials. *Phys. Rev. B* **54,** 1703–1710, http://dx.doi.org/10.1103/PhysRevB.54.1703 (1996).
39. Krack, M. Pseudopotentials for H to Kr optimized for gradient-corrected exchange-correlation functionals. *Theor Chem Acc* **114,** 145–152, doi: 10.1007/s00214-005-0655-y (2005).
40. VandeVondele, J. & Hutter, J. Gaussian basis sets for accurate calculations on molecular systems in gas and condensed phases. *J. Chem. Phys.* **127,** 114105(1)-114105(9), doi: 10.1063/1.2770708 (2007).
41. Perdew, J., Burke, K. & Matthias, H. Generalized Gradient Approximation Made Simple. *Phys. Rev. Lett.* **77,** 3865–3868, http://dx.doi.org/10.1103/PhysRevLett.77.3865 (1996).
42. Grimme, S., Antony, J., Ehrlich, S. & Krieg, H. A consistent and accurate ab initio parametrization of density functional dispersion correction (DFT-D) for the 94 elements H-Pu. *J. Chem. Phys.* **132,** 154104(1)-154104(19), doi: 10.1063/1.3382344 (2010).
43. Ji, Y., Wang, B. & Luo, Y. Location of Trapped Hole on Rutile-TiO_2(110) Surface and Its Role in Water Oxidation. *J. Phys. Chem. C* **116,** 7863–7866, doi: 10.1021/jp300753f (2012).
44. Henkelman, Uberuaga, G., Jónsson, B. P. & Hannes. A climbing image nudged elastic band method for finding saddle points and minimum energy paths. *J. Chem. Phys.* **113,** 9901–9904, http://dx.doi.org/10.1063/1.1329672 (2000).
45. Di Valentin, C., Pacchioni, G. & Selloni, A. Electronic Structure of Defect States in Hydroxylated and Reduced Rutile TiO_2(110) Surfaces. *Phys. Rev. Lett.* **97,** 166803(1)–166803(4), doi: 10.1103/PhysRevLett.97.166803 (2006).

Acknowledgements

This work was supported by the National Natural Science Foundation of China (Nos. 51572016, 51222212). This research work is supported by a Tianhe-2JK computing time award at the Beijing Computational Science Research Center (CSRC). Special Program for Applied Research on Super Computation of the NSFC-Guangdong Joint Fund (the second phase).

Author Contributions

The idea was conceived by L.L. The simulation was performed by W.Y. The data analyses were performed by W.Y., B.W., S.B., M.K., M.L. and L.L. This manuscript was written by W.Y. and L.L. All authors discussed the results and contributed to the paper.

Additional Information

Competing financial interests: The authors declare no competing financial interests.

How to cite this article: Yin, W.-J. *et al.* The Effect of Excess Electron and hole on CO_2 Adsorption and Activation on Rutile (110) surface. *Sci. Rep.* **6**, 23298; doi: 10.1038/srep23298 (2016).